Journal of Power Sources 205 (2012) 244–251

Contents lists available at ScienceDirect

Journal of Power Sources

journal homepage: www.elsevier.com/locate/jpowsour

# Degradation of the elastomeric gasket material in a simulated and four accelerated proton exchange membrane fuel cell environments

Guo Li, Jinzhu Tan, Jianming Gong*

*School of Mechanical and Power Engineering, Nanjing University of Technology, Nanjing, Jiangsu 210009, China*

ARTICLE INFO

*Article history:*
Received 25 May 2011
Received in revised form 25 June 2011
Accepted 27 June 2011
Available online 2 July 2011

*Keywords:*
Chemical degradation
Elastomeric gasket
Silicone rubber
Fuel cell
Simulated environment
X-ray photoelectron spectroscopy

ABSTRACT

Long-term stability and durability of gaskets in Proton Exchange Membrane (PEM) fuel cell are critical to both sealing and the electrochemical performance of the PEM fuel cell. In this paper, the time-dependent chemical degradation of the silicone rubber, which is one of the potential gasket materials for PEM fuel cells, is studied in a simulated PEM fuel cell environment and four accelerated durability test (ADT) media for short-term aging tests at 70 °C. The weight loss of samples is monitored. The optical microscopy is used to show the topographical changes on the sample surface. Attenuated total reflection Fourier transform infrared (ATR-FTIR) spectroscopy and X-ray photoelectron spectroscopy (XPS) are employed to study the surface chemistry of the samples before and after exposure to the test environments over time. The results show that the weight loss increases with the exposure time. The optical microscopy reveals that the surface conditions of the samples changes from initially smooth to rough, crack appearance and finally crack propagation. The ATR-FTIR and XPS results show that the surface chemistry changes significantly via de-crosslinking and chain scission in the backbone for the samples exposed to the environments over time.



## 1. Introduction

In order to keep the reactant gases (hydrogen and oxygen) within their respective regions, Polymer Electrolyte Membrane (PEM) fuel cell stack requires elastomeric gaskets in each cell. The gaskets are exposed to acidic environment, humid air and hydrogen, and subjected to mechanical compressive load. If any elastomeric gasket material ages or fails in PEM fuel cells, the gasket loses its elastic property and seal functionality. Furthermore, if any gasket degrades, the reactant gases may leak or mix each other directly during operation, and this not only decreases the performance of PEM fuel cell, but also poses a safety concern [1]. Therefore, the degradation of the elastomeric gasket material in PEM fuel cell environment over time is an issue for PEM fuel cells.

In open literatures, there are many reports in which the major emphasis is on both thermal and irradiative degradation on polymeric materials [2–5]. For instance, Wang et al. [4] studied the aging behavior and thermal degradation of fluoroelastomer reactive blends with poly-phenol hydroxy EPDM. Youn and Huh [5] examined the surface degradation of silicone rubber and EPDM under accelerated ultraviolet weathering conditions. Mitra et al. [6–8] investigated the chemical degradation of cross-linked EPDM rubber in a 20% $Cr/H_2SO_4$ acidic environment and that of fluoroelastomer in an alkaline environment, respectively. A review on the effects and degradation process of silicones in outdoor environments can be found in Graiver et al. [9]. Hsu et al. [10] studied the moisture-related degradation of EPDM by electrical and SEM methods. There are also many reports concerning the degradation of some components in PEM fuel cells [11–16]. For example, Akiyama et al. [11] studied the degradation process of polymer electrolyte by solution analysis. Yuan et al. [12] studied the performance of the fuel cell changing with various degree of degradation of MEA by situ diagnosis. Wu and Fuller [16] modeled the degradation of Pt/C catalyst in fuel cell. Lin et al. [17] studied the chemical degradation of copolymeric resin, liquid silicone rubber, fluorosilicone rubber, EPDM and fluoroelastomer copolymer in a simulated and an accelerated PEM fuel cell environment at 80 °C. Tan et al. [18–24] studied the chemical and mechanical degradation of silicone rubber, fluoroelastomer and EPDM materials exposed to a simulated PEM fuel cell environment and one accelerated durability test solution at the temperature of 60 °C and 80 °C.

In this paper, the chemical degradation of the silicone rubber material, which is widely used as sealing material in lots of industrial applications including PEM fuel cells due to its low cost and ease in fabrication, was investigated in a simulated and four accelerated PEM fuel cell environments. The aim of the present study is to investigate the degree of degradation and its mechanisms for the silicone rubber samples exposed to five acidic test solutions at the temperature of 70 °C. The regular solution (RS) [18,19] similar to the actual PEM fuel cell environment and four accelerated

* Corresponding author. Tel.: +86 25 83587291; fax: +86 2583587291.
*E-mail address:* gongjm@njut.edu.cn (J. Gong).

0378-7753/$ – see front matter © 2012 Published by Elsevier B.V.
doi:10.1016/j.jpowsour.2011.06.092

durability test (ADT) solutions were prepared. The ADT solutions were used for the short-term, accelerated aging tests on the silicone rubber. The weight changes were monitored on the samples at selected exposure time. The topographical changes on the surface of the samples were examined using optical microscopy and the chemistry changes of the silicone rubber before and after exposure over time were studied by ATR-FTIR spectroscopy and XPS.

## 2. Experiments

### 2.1. Material and test environments

The silicone rubber studied in the work is a commercial elastomeric material. The rubber is a two-part formulation liquid injection molded material. It mainly contains polydimethylsilicoxane with vinyl functionalities in part A and polydimethylsilicoxane with hydrosilylation functionalities in part B. The part A and part B (1:1) combined and heated to crosslink under the platinum catalyzed reaction. The crosslinking mechanism is hydrosilylation. The fillers inside the material mainly include silica, quartz, calcium carbonate, etc.

Five solutions were used to age the material. The first solution is termed the "Regular" solution, which is similar to the real PEM fuel cell environment [18,19]. 48% HF and 98% $H_2SO_4$ were dissolved in balance reagent water to make the test solution. The composition of the regular solution is 12.5 ppm $H_2SO_4$, 1.8 ppm HF [18,19] and reagent grade water having 18 Mega Ohm (MΩ) resistance.

The four ADT solutions, namely, ADT1, ADT2, ADT3 and ADT4 solution, were used for short-term accelerated aging tests. Again, 48% HF and 98% $H_2SO_4$ were dissolved in balance reagent water to make the ADT solutions. The composition of the ADT1 solution is 1 M $H_2SO_4$, 10 ppm HF [18,19] and reagent grade water having 18 MΩ resistance. The composition of the ADT2 solution is 1 M $H_2SO_4$, 30 ppm HF and reagent grade water having 18 MΩ resistance. The composition of the ADT3 solution is 1 M $H_2SO_4$, 50 ppm HF and reagent grade water having 18 MΩ resistance. The composition of the ADT4 solution is 1 M $H_2SO_4$, 100 ppm HF and reagent grade water having 18 MΩ resistance.

The test temperature was selected at 70 °C which is close to the operating temperature of actual PEM fuel cells.

### 2.2. Aging and characterization methods

A sheet of silicone rubber was cut into 10 rectangular-shaped samples. The dimensions of the samples are 10 mm in length, 10 mm in width and 6 mm in thickness. The samples were divided into 5 groups. Each group included 2 samples. The samples were placed in the bottles containing the regular solution and four ADT solutions, respectively. The bottles were then put in an oven with the temperature of 70 °C. The aged samples were taken out of the test bottles at selected times for examination. In order to avoid the effect of the remaining solution on the sample surface on the test results, the surface of the sample was cleaned using reagent grade water having 18 MΩ resistance to remove the excess acids and made dry at room temperature before the analysis.

The changes in weight of the samples were monitored by microelectronic balance. The optical microscope was used to examine the surface topographical changes at selected times. The ATR-FTIR spectroscopy was employed to study the surface chemistry of the samples before and after exposure to the test environments using a Nexus Model 670 Instrument (Nicolet Instrument Corporation) which runs with 32 scans at a resolution of 0.1 $cm^{-1}$. The infrared radiation (IR) penetrates the surface of the samples to approximately 1 μm.

The XPS analysis was conducted using a Thermo Fisherscientific K-Alpha spectrometer with monochromatic Al Kα X-ray source. The survey spectra in the range of 0–1200 eV were recorded in 1 eV step for each sample. Atomic concentrations of each element were calculated by determining the relevant integral peak intensities. High-resolution analysis was performed in the carbon 1s (C 1s) and the silicon 2p (Si 2p) regions. The spectra were deconvoluted by curve-fitting. The high-resolution spectra were recorded in 0.1 eV steps from which the detailed compositions were calculated.

## 3. Results and discussion

### 3.1. Weight change

The silicone rubber samples were taken out from the oven for tests at selected times. The surface of the samples was cleaned using reagent grade water having 18 MΩ resistance to remove the excess acids and made dry at room temperature before analysis. The weight of the samples before and after exposure was monitored by a micro-electronic balance. The percent weight loss, $W_L$, was calculated by the following equation:

$$W_L\ (\%) = \frac{W_2 - W_1}{W_1} \times 100 \quad (1)$$

where $W_1$ is the initial weight of the sample in air, and $W_2$ is the weight of the aged sample in air.

Fig. 1 shows the weight loss with exposure time under various test conditions. It can be seen that the weight was lost in the test environments over time. The weight of the samples exposed to the regular solution did not decreased apparently, while the weight of the samples exposed to the ADT solutions decreased remarkably. The higher the concentration of the acid in the test solutions, the more the weight lost. These results show that both exposure time and exposure environments had significant effect on the weight loss for the samples exposed to the environments.

Test results of percent weight loss per hour are listed in Table 1. It can be seen that the weight loss rate increased with the increase of the concentration of acidic solution. Higher concentration of the acid in the ADT solutions apparently corroded more out of the material in the same exposure time.

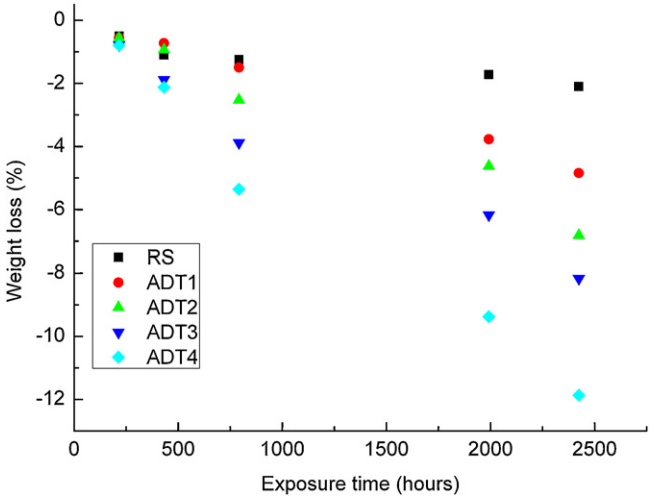


**Fig. 1.** Weight loss versus exposure time.

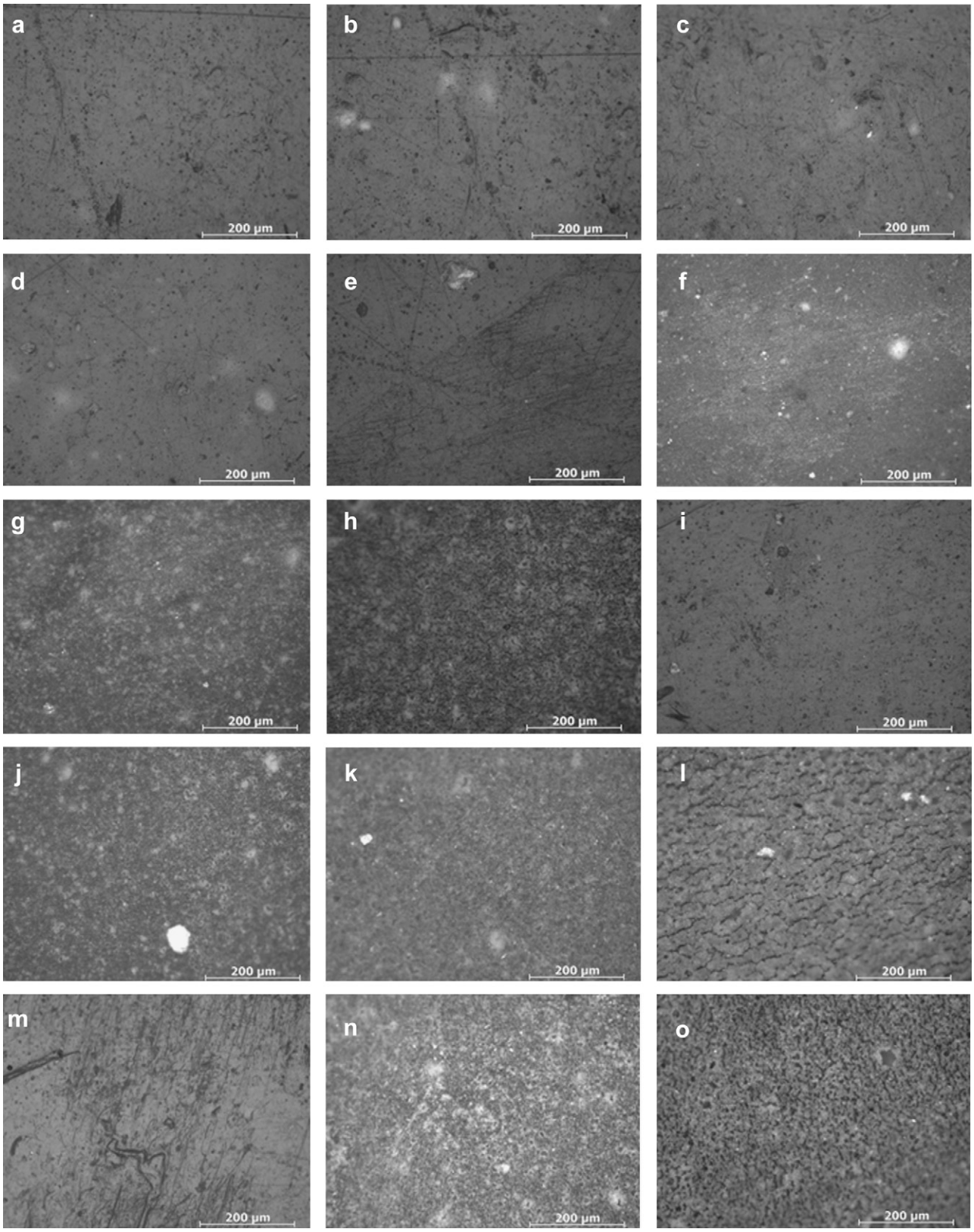


**Fig. 2.** Topographical photos of the surface from the samples in test solutions. (a) Before exposure, (b) after 216 h, (c) after 432 h, (d) after 792 h, (e) before exposure, (f) after 216 h, (g) after 432 h, (h) after 792 h, (i) before exposure, (j) after 216 h, (k) after 432 h, (l) after 792 h, (m) before exposure, (n) after 216 h, (o) after 432 h, (p) after 792 h, (q) before exposure, (r) after 216 h, (s) after 432 h and (t) after 792 h.

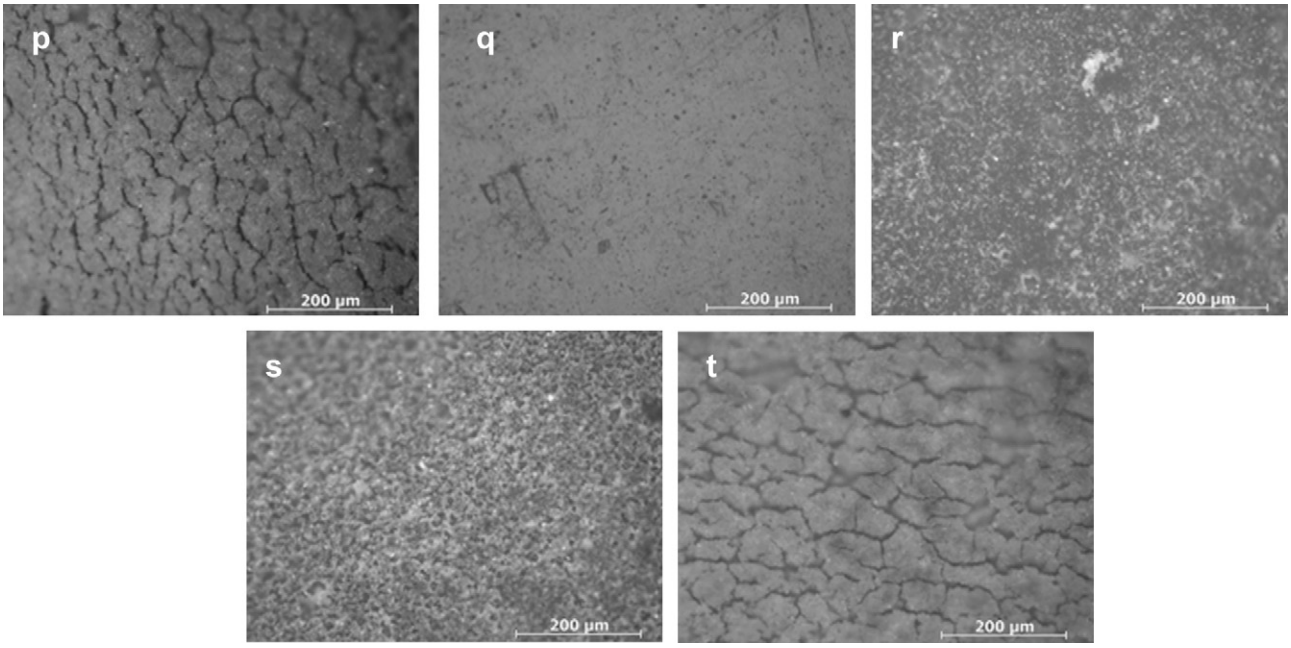


**Fig. 2.** (*Continued.*)

### 3.2. Microscopy

The topographical changes on the surface of the samples before and after 792 h exposure to the test solutions at 70 °C were observed by optical microscopy. The optical micrographs for the samples are shown in Fig. 2. The magnification used was 200×. The photos (a)–(d) in Fig. 2 represent the surface micrographs of the samples exposed to the regular solution. The photos (e)–(h), (i)–(l),

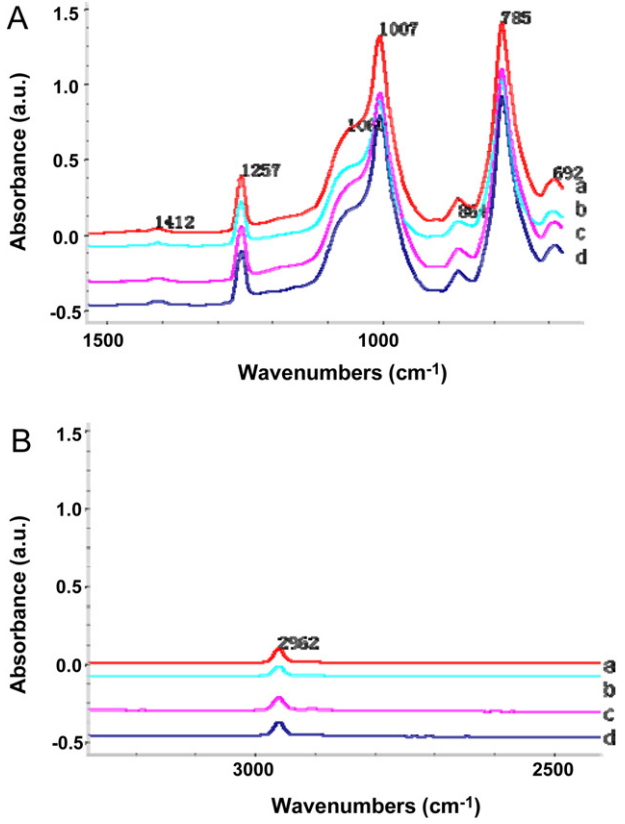


**Fig. 3.** Comparison of ATR-FTIR test results for the sample exposed to regular solution at 70 °C: (A) ATR-FTIR spectra from 650 to 1500 $cm^{-1}$; (B) ATR-FTIR spectra from 2500 to 3500 $cm^{-1}$; (a) without exposure, after (b) 216 h exposure, (c) 432 h exposure, (d) 792 h exposure.

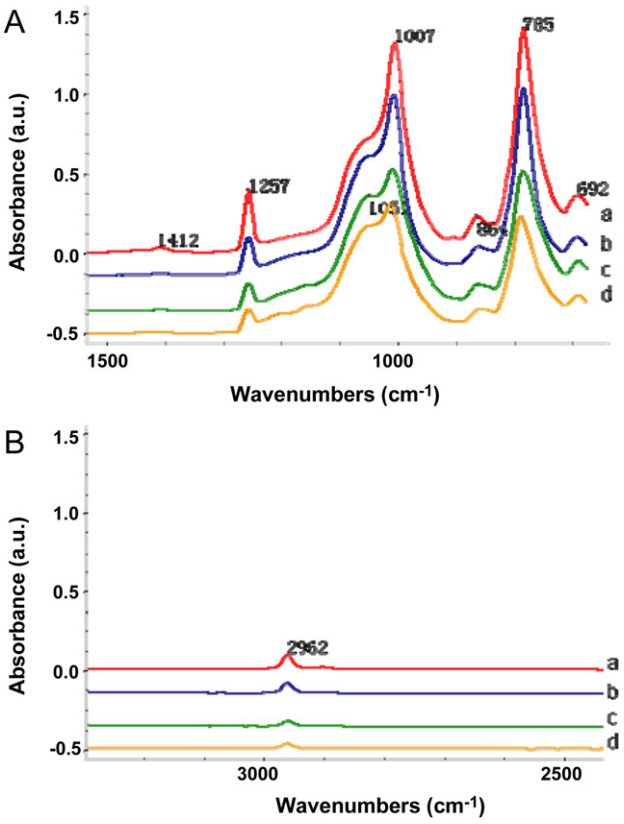


**Fig. 4.** Comparison of ATR-FTIR test results for the sample exposed to ADT1 solution at 70 °C: (A) ATR-FTIR spectra from 650 to 1500 $cm^{-1}$; (B) ATR-FTIR spectra from 2500 to 3500 $cm^{-1}$; (a) without exposure, after (b) 216 h, (c) 432 h, (d) 792 h exposure.

**Table 1**
Percent weight loss per hour of the samples in all test environments.

| Exposed time (h) | Exposed environment | | | | |
|---|---|---|---|---|---|
| | RS | ADT1 | ADT2 | ADT3 | ADT4 |
| 216 | −0.00231 | −0.00256 | −0.00259 | −0.00362 | −0.00366 |
| 432 | −0.00279 | −0.00079 | −0.00174 | −0.00511 | −0.00616 |
| 792 | −0.00039 | −0.00214 | −0.0044 | −0.00554 | −0.00898 |
| 1992 | −0.0004 | −0.0019 | −0.00175 | −0.00191 | −0.00335 |
| 2424 | −0.00088 | −0.00248 | −0.00509 | −0.00463 | −0.00576 |

(m)–(p) and (q)–(t) represent the surface micrographs of the samples exposed to ADT1 solution, ADT2 solution, ADT3 solution and ADT4 solution, respectively.

Optical micrographs (a) through (d) in Fig. 2 show the surface topographical changes of the silicone rubber before and after exposure to the regular solution for 216 h, 432 h and 792 h, respectively. It can be seen that the surface condition of the samples exposed to the regular solution did not change significantly. No cracks were observed and the surface almost kept smooth. The result shows that the degradation was not obvious for the samples after exposure to the solution up to 792 h.

Optical micrographs (e) through (h) in Fig. 2 show the surface topographical changes of the sample before and after exposure to ADT1 solution for 216 h, 432 h and 792 h, respectively. It can be seen that the surface of the sample became rough after 792 h exposure.

Optical micrographs (i) through (l) in Fig. 2 show the typical surface condition of the sample before and after exposure to ADT2 solution for 216 h, 432 h and 792 h, respectively. The surface became rough after 216 h exposure (see Fig. 2(j)). The cracks were observed apparently on the surface of the sample after exposure of 792 h (see Fig. 2(l)).

Optical micrographs (m) through (p) in Fig. 2 show the surface topographical changes of the sample before and after exposure to ADT3 solution for 216 h, 432 h and 792 h, respectively. The surface became rough after 216 h exposure. Some spot corrosion occurred after exposure of 432 h. The cracks initiated and propagated on the surface of the samples after exposure of 792 h. The extent of surface damage in ADT3 solution is more severe compared to ADT2 solution under identical conditions (see Fig. 2(p) for ADT3 solution and Fig. 2(l) for ADT2 solution).

Optical micrographs (q) through (t) in Fig. 2 show the surface topographical changes of samples before and after exposure to ADT4 solution for 216 h, 432 h and 792 h, respectively. The surface became rough after 216 h exposure. Some spot corrosion also occurred after exposure of 432 h. The cracks initiated and propagated on the surface of the samples after exposure for 792 h. The trend of surface damage in the ADT4 solution is similar to that in

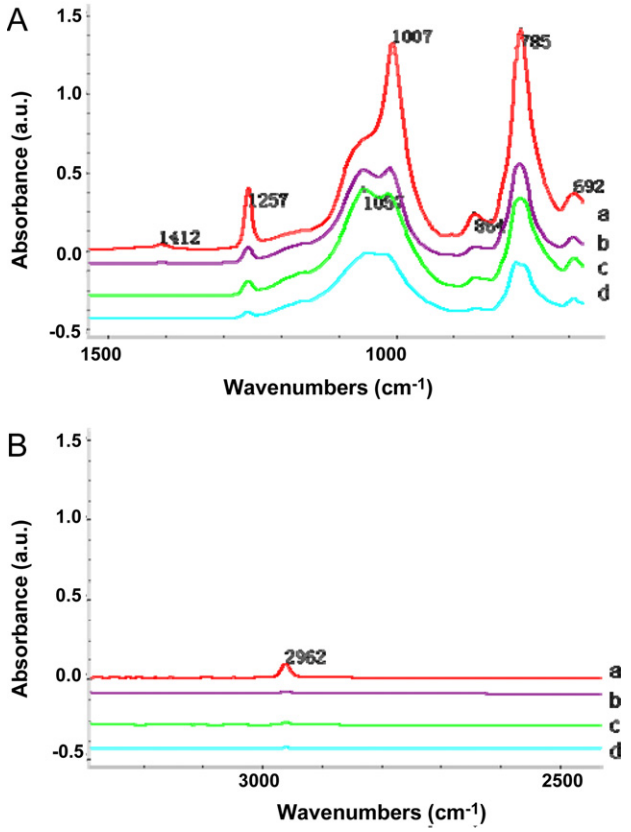


**Fig. 5.** Comparison of ATR-FTIR test results for the sample exposed to ADT2 solution at 70 °C: (A) ATR-FTIR spectra from 650 to 1500 $cm^{-1}$; (B) ATR-FTIR spectra from 2500 to 3500 $cm^{-1}$; (a) without exposure, after (b) 216 h, (c) 432 h, (d) 792 h exposure.

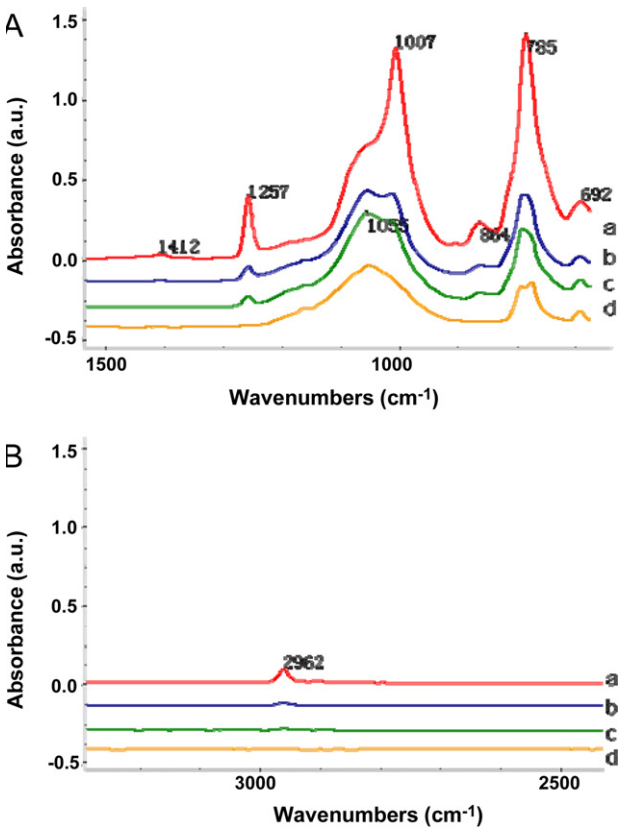


**Fig. 6.** Comparison of ATR-FTIR test results for the sample exposed to ADT3 solution at 70 °C: (A) ATR-FTIR spectra from 650 to 1500 $cm^{-1}$; (B) ATR-FTIR spectra from 2500 to 3500 $cm^{-1}$; (a) without exposure, after (b) 216 h, (c) 432 h, (d) 792 h exposure.

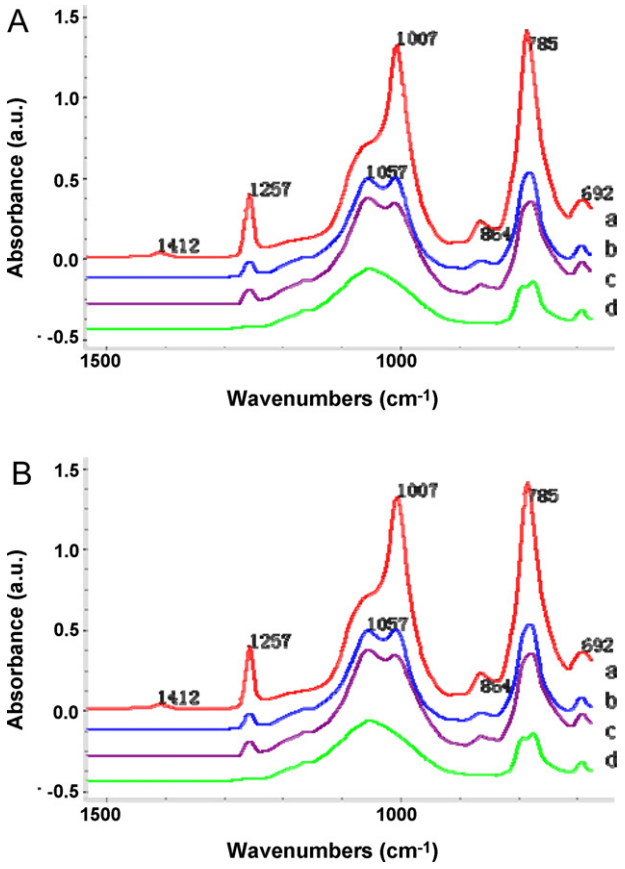


**Fig. 7.** Comparison of ATR-FTIR test results for the sample exposed to ADT4 solution at 70 °C: (A) ATR-FTIR spectra from 650 to 1500 $cm^{-1}$; (B) ATR-FTIR spectra from 2500 to 3500 $cm^{-1}$; (a) without exposure, after (b) 216 h, (c) 432 h, (d) 792 h exposure.

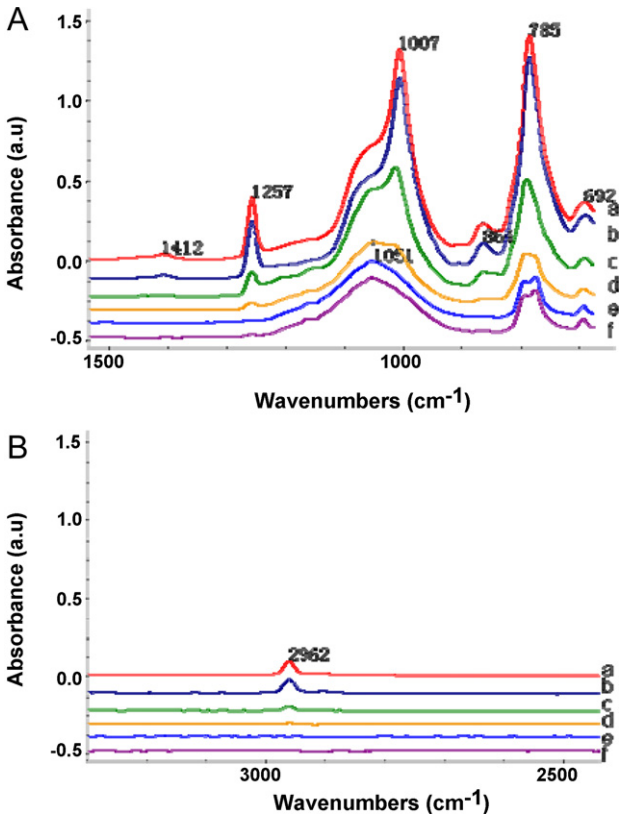


**Fig. 8.** Comparison of ATR-FTIR test results for the sample exposed to all test solutions for 33days at 70 °C: (A) ATR-FTIR spectra from 650 to 1500 $cm^{-1}$; (B) ATR-FTIR spectra from 2500 to 3500 $cm^{-1}$; (a) without exposure, after (b) 792 h exposure in RS, (c) 792 h exposure in ADT1, (d) 792 h exposure in ADT2, (e) 792 h exposure in ADT3, (f) 792 h exposure in ADT4.

the ADT3 solution (see Fig. 2(t) for ADT4 solution and Fig. 2(p) for ADT3 solution).

From the optical microscopy results, it can be concluded that (a) the surface damage of the silicone rubber sample in ADT solutions is more severe compared to the regular solution under identical condition, (b) the surface topography of the sample exhibits time-dependent degradation, and (c) the concentration of the hydrofluoric acidic solution has significant effect on the degradation.

### 3.3. ATR-FTIR

ATR-FTIR was performed on the silicone rubber samples before and after exposure to the test solutions to study the chemistry change. Figs. 3–8 show the ATR-FTIR results for the samples exposed to RS, ADT1, ADT2, ADT3 and ADT4 solutions at 70 °C up to 792 h, respectively. The spectra a, b, c and d in Figs. 3–7 represent the samples before and after exposure to the various solutions for 216 h, 432 h and 792 h, respectively. The spectra a, b, c, d, e and f in Fig. 8 represent the samples before exposure and after exposure to RS, ADT1, ADT2, ADT3 and ADT4 solutions for 792 h at 70 °C, respectively.

The strongest and broadest peaks for the unexposed samples (see Figs. 3(A-a)–8(A-a)) are between 1007 $cm^{-1}$ and 1060 $cm^{-1}$ and there are other peaks at 785 $cm^{-1}$, 1257 $cm^{-1}$, 864 $cm^{-1}$, 692 $cm^{-1}$ and 2962 $cm^{-1}$. The peaks at 1007–1060 $cm^{-1}$ are due to the stretching vibrations of Si–O–Si present in the silicone rubber backbone. The peaks at 785 $cm^{-1}$ are probably from vibrational coupling between the Si–C stretching mode and the $CH_3$ rocking mode for the Si–$CH_3$ group. The peaks at 1257 $cm^{-1}$ and 864 $cm^{-1}$ are from the bending vibration of Si–$CH_3$ and the rocking vibration of Si–$CH_3$, respectively. The peaks near 1412 $cm^{-1}$ are from the rocking vibration of –$CH_2$– as a part of the silicone rubber crosslinked domain. The peaks at 692 $cm^{-1}$ and 2962 $cm^{-1}$ are from the stretching vibration of $CH_3$. The correspondence between the wavenumber and the vibration mode is from the handbook [25].

For silicone rubber samples in regular solution (see Fig. 3(A) and (B)), the intensity of all peaks had little changes. This result indicates that the surface chemistry on the silicone rubber did not changed evidently in regular solution. The result is in agreement with that observed by optical microscope.

For silicone rubber samples exposed to ADT1 solution (see Fig. 4(A) and (B)), the intensity of the peaks between 1007 $cm^{-1}$ to 1060 $cm^{-1}$, 785 $cm^{-1}$, 1257 $cm^{-1}$ and 2962 $cm^{-1}$ decreased with the exposure time. The intensity of the peaks at 864 $cm^{-1}$ and 692 $cm^{-1}$ decreased gradually and the peak at 1412 $cm^{-1}$ is almost disappeared after the exposure of 792 h.

For silicone rubber samples exposed to ADT2 solution (see Fig. 5(A) and (B)), the intensity of the peaks between 1007 $cm^{-1}$ to 1060 $cm^{-1}$, 785 $cm^{-1}$, 1257 $cm^{-1}$ and 692 $cm^{-1}$ decreased sharply with exposure time. The peak at 864 $cm^{-1}$ almost disappeared after 792 h exposure. The peaks at 1412 $cm^{-1}$ and 2962 $cm^{-1}$ also disappeared after 432 h exposure.

For silicone rubber samples exposed to ADT3 solution (see Fig. 6(A) and (B)), the intensity of the peaks between 1007 $cm^{-1}$ to 1060 $cm^{-1}$, 785 $cm^{-1}$, 1257 $cm^{-1}$, 864 $cm^{-1}$ and 2962 $cm^{-1}$ decreased dramatically after 216 h exposure. The intensity of the peaks at 692 $cm^{-1}$ decreased over time. The peak at 1257 $cm^{-1}$

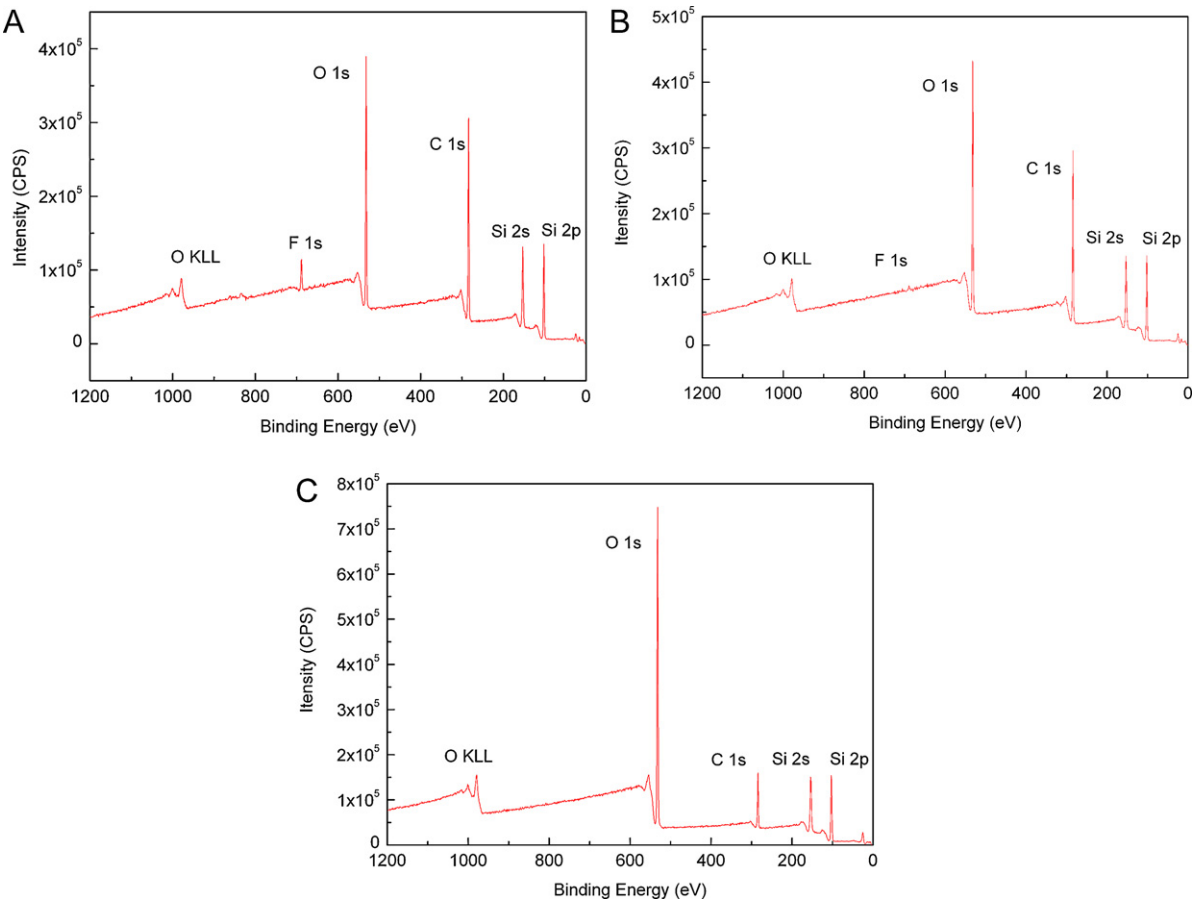


**Fig. 9.** XPS survey spectra for silicone rubber samples before and after exposure to test solutions at 70 °C: (a) before exposure, (b) 1992 h exposure in regular solution, (c) 1992 h exposure in ADT2.

disappeared after 792 h exposure. The peaks at 1412 $cm^{-1}$ and 2962 $cm^{-1}$ also disappeared after 432 h exposure.

For silicone rubber samples exposed to ADT4 solution (see Fig. 7(A) and (B)), the intensity of the peaks between 1007 $cm^{-1}$ to 1060 $cm^{-1}$, 785 $cm^{-1}$, 1257 $cm^{-1}$, 864 $cm^{-1}$ and 2962 $cm^{-1}$ decreased dramatically after 216 h exposure. The intensity of the peaks at 692 $cm^{-1}$ decreased over time. The peaks at 1257 $cm^{-1}$ and 2962 $cm^{-1}$ disappeared after 792 h exposure. The peak at 1412 $cm^{-1}$ disappeared after 432 h exposure.

From Fig. 8(A) and (B), it can be seen that the intensity of all peaks of the samples in regular solution did not changed apparently. However, the intensity of the peaks of the samples in all the ADT solutions changed significantly. The intensity of peaks of the samples in the ADT4 solution decreased more compared to the ADT1 solution under identical conditions. The results show that the concentration of the hydrofluoric acidic solution had significant effect on the chemical degradation for the samples. The result is agreement with that from the optical microscopy.

The ATR-FTIR results indicate that the intensities of the peaks at 2962 $cm^{-1}$, 692 $cm^{-1}$, 1412 $cm^{-1}$, 1257 $cm^{-1}$, 864 $cm^{-1}$, 1007–1060 $cm^{-1}$, and 785 $cm^{-1}$ decreased for the samples exposed to the ADT solutions over time. The concentration of the acid in the ADT solutions had significant effect on the degradation for the samples exposed to the environments. The higher the concentration of the acid in ADT solutions, the more the material degraded. In addition, it is found that there were the similar trends for the samples exposed to the four ADT solutions under the identical conditions. The results reveal that the degradation and degradation mechanisms are similar for the samples exposed to the test environments.

It can be concluded from ATR-FTIR results that there were significant chemical changes in silicone rubber backbone and the crosslink domain for the silicone rubber samples exposed to the test environments over time. The degradation mechanisms of the silicone rubber could be due to de-crosslinking via hydrolysis of crosslink sites and chain scissoring in the backbone in the test environments. The chemical changes in the silicone rubber backbone could be due to the attack of the Si–O–Si by strong acid, especially Fluoric acid, to form Si–OH. And then the Si–OH could be converted to Si–O [1,26–28]. Although the main chain Si–O–Si in silicone rubber is stable, the Si–O–Si can be attacked in strong acidic environment and this caused significant chemical change [1,26–28].

### 3.4. X-ray photoelectron spectroscopy (XPS)

XPS is a surface sensitive analysis method to elucidate the surface chemicals. In present study, XPS was employed to observe qualitative and quantitative information on the surface of the silicone rubber samples before and after 1992 h exposure to regular solution and ADT2 solution at 70 °C as shown in Fig. 9(a)–(c), respectively.

The spectra (see Fig. 9(a)–(c)) revealed the presence of carbon (C), oxygen (O), silicon (Si) and small amount of fluorine (F). The atomic concentrations of these elements are given in Table 2. The

**Table 2**
Surface atomic concentration of each element and ratios of atomic concentrations of O and C to Si for silicone rubber samples before and after exposure to ADT2 solution at 70 °C.

| Samples | Atomic concentration (at.%) | | | | Rations to Si | |
|---|---|---|---|---|---|---|
| | C | O | Si | F | C/Si | O/Si |
| Before exposure | 46.3 | 25.49 | 27.74 | 0.64 | 1.663 | 0.919 |
| 1992 h exposure in RS | 44.01 | 27.1 | 28.28 | 0.6 | 1.556 | 0.958 |
| 1992 h exposure in ADT2 | 21.2 | 45.72 | 32.28 | 0.8 | 0.657 | 1.416 |

presence of F may result from the environment occurred on the surface of the sample. From Fig. 9, it can be observed that the carbon peak decreased and the oxygen peak increased with exposure time. Especially, the carbon peak and oxygen peak changed significantly for samples exposed to ADT2 solution. Table 2 also shows the ratios of concentration (C/Si and O/Si) for samples before and after exposure over time. As shown in Table 2, the C/Si ratio decreased significantly with increasing exposure time and acidic concentration. This could be due to that the methyl group on the silicon atom was attacked and oxidized to form the Si–O bonds. The increase of O/Si ratio with exposure time may indicate that the chain in the backbone (–Si–O–Si–) was attacked and broken.

These changes of chemical compositions reflect the chemical degradation of the materials exposed to the test environments. The degradation proceeded via de-cross-linking and chain scission in the backbone accompanied with the damage of the fillers in the material. The degradation may affect the mechanical properties of the gasket material, the electrochemical performance, and therefore the long-term durability of PEM fuel cell. The XPS results are in agreement with the FTIR observations.

## 4. Conclusions

Degradation of the silicone rubber, a commercial available elastomeric gasket material used as sealing in fuel cell, was studied in a simulated PEM fuel cell environment and four ADT solutions. The conclusions obtained are as follows:

(1) The concentration of the acid in test solutions has a significant effect on the degradation by weight loss. The weight loss increased with the concentration of the acidic solution.
(2) Optical microscopy shows that surface topography of the sample exhibited time-dependent degradation, and the degradation started from surface roughness and finally cracks for the samples after exposure to the test environments.
(3) ATR-FTIR spectrometry and XPS results indicate that the surface chemistry changed significantly as an indication of the chemical degradation of the silicone rubber material for the exposure to the environments. The concentration of the hydrofluoric (HF) acidic solution has an important effect on the chemical degradation of the silicone rubber. The degradation mechanisms of the silicone rubber could proceed via de-crosslinking through hydrolysis of crosslink sites and chain scissoring in the backbone.
(4) Current work is to show the chemical degradation and degradation mechanisms on the silicone rubber material in a simulated and four accelerated PEM fuel cell environments. The chemical degradation may affect not only the mechanical properties of the material, but also electrochemical performance of the fuel cell. Studies on the degradation in mechanical properties of the material after exposure to the environments is under investigation and will be reported later.

## Acknowledgements

The work is sponsored by the Specialized Research Fund for the Doctoral Program of Higher Education of China (200802910004), the Natural Science Foundation of Jiangsu Province in China (BK2009362), and the Natural Science Foundation for Colleges and Universities in Jiangsu Province of China (08KJB430005). The work is also supported by the Project-sponsored by the Scientific Research Foundation for the Returned Oversea Chinese Scholars, State Education Ministry, and the innovation Program for Graduate Students in Nanjing University of Technology (BSCX200904). The assistance from Professor Y.J. Chao is acknowledged.

## References

[1] J. Tan, Y.J. Chao, X. Li, J.W. Van Zee, J. Power Sources 172 (2) (2007) 782–789.
[2] R.S. Rajeev, S.K. De, A.K. Bhowmick, B. John, Polym. Degrad. Stab. 79 (3) (2003) 449–463.
[3] T. Ueno, E. Nakashima, K. Takedab, Polym. Degrad. Stab. 95 (9) (2001) 1862–1869.
[4] Y. Wang, L. Liu, Y. Luo, D. Jia, Polym. Degrad. Stab. 94 (3) (2009) 443–449.
[5] B.H. Youn, C.S. Huh, IEEE Trans. Dielect. Elect. Insul. 12 (5) (2005) 1015–1024.
[6] S. Mitra, A. Ghanbari-Siahkali, P. Kingshott, H.K. Rehmeier, H. Abildgaard, K. Almdal, Polym. Degrad. Stab. 91 (2006) 69–80.
[7] S. Mitra, A. Ghanbari-Siahkali, P. Kingshott, H.K. Rehmeier, H. Abildgaard, K. Almdal, Polym. Degrad. Stab. 91 (2006) 81–93.
[8] S. Mitra, A. Ghanbari-Siahkali, P. Kingshott, K. Almdal, H.K. Rehmeier, A.G. Christensen, Polym. Degrad. Stab. 83 (2004) 195–206.
[9] D. Graiver, K.W. Farminer, R. Narayan, J. Polym. Environ. 11 (4) (2003) 129–136.
[10] Y.T. Hsu, K.S. Chang-Liao, T.K. Wang, C.T. Kuo, Polymer Polym. Degrad. Stab. 91 (10) (2006) 2357–2364.
[11] Y. Akiyama, H. Sodaye, Y. Shibahara, Y. Honda, S. Tagawa, S. Nishijima, J. Power Sources 195 (18) (2010) 5915–5921.
[12] X. Yuan, S. Zhang, H. Wang, J. Wu, J.C. Sun, R. Hiesgen, K. Andreas Friedrich, M. Schulze, A. Haug, J. Power Sources 195 (22) (2010) 7594–7599.
[13] M. Jung, K.A. Williams, J. Power Sources 196 (5) (2011) 2717–2724.
[14] C. Chen, G. Levitin, D.W. Hess, T.F. Fuller, J. Power Sources 169 (2) (2007) 288–295.
[15] S. Vengatesan, M.W. Fowler, X. Yuan, H. Wang, J. Power Sources 196 (11) (2011) 5045–5052.
[16] B. Wu, T.F. Fuller, J. Power Sources 178 (1) (2008) 188–196.
[17] C. Lin, C. Chien, J. Tan, Y.J. Chao, J.W. Van Zee, J. Power Sources 196 (2011) 1955–1966.
[18] J. Tan, Y.J. Chao, W.K. Lee, C.S. Smith, J.W. Van Zee, C.T. Williams, Proceedings of the 4th International Conference on Fuel Cell Science, Engineering and Technology, June 19–21, Irvine, CA, 2006.
[19] J. Tan, Y.J. Chao, J.W. Van Zee, W.K. Lee, Mater. Sci. Eng. A 445–446 (2007) 669–675.
[20] J. Tan, Y.J. Chao, M. Yang, C.T. Williams, J.W. Van Zee, J. Mater. Eng. Perform. 17 (2008) 785–792.
[21] J. Tan, Y.J. Chao, J.W. Van Zee, W.K. Lee, Mater. Sci. Eng. A 496 (2008) 464–470.
[22] J. Tan, Y.J. Chao, H. Wang, J. Gong, J.W. Van Zee, Polym. Degrad. Stab. 94 (2009) 2072–2078.
[23] J. Tan, Y.J. Chao, X. Li, J.W. Van Zee, W.K. Lee, J. Fuel Cell Sci. Technol. 6 (4) (2009) 0410171–0410179.
[24] J. Tan, Y.J. Chao, M. Yang, W.K. Lee, J.W. Van Zee, Int. J. Hydrogen Energy 36 (2011) 1846–1852.
[25] D. Lin-Vien, N.B. Colthup, W.G. Fateley, J.G. Grasselli, The Handbook of Infrared and Raman Characteristic Frequencies of Organic Molecules, Academic Press, Boston, 1991.
[26] N. Yoshimura, S. Kumagai, S. Nishimura, IEEE Trans. Dielect. Elect. Insul. 6 (5) (1999) 632–650.
[27] F. Delor-Jestin, N.S. Tomer, R.P. Singh, J. Lacoste, E-Polymer 5 (2006) 1–13.
[28] W. Noll, Chemistry and Technology of Silicone, Academic Press, Boston, 1968.